



## Discover Generics

Cost-Effective CT & MRI Contrast Agents



WATCH VIDEO

# AJNR

### **3D Time-Resolved Contrast-Enhanced Cerebrovascular MR Angiography with Subsecond Frame Update Times Using Radial $k$ -Space Trajectories and Highly Constrained Projection Reconstruction**

This information is current as of June 17, 2025.

Y. Wu, N. Kim, F.R. Korosec, A. Turk, H.A. Rowley, O. Wieben, C.A. Mistretta and P.A. Turski

*AJNR Am J Neuroradiol* 2007, 28 (10) 2001-2004

doi: <https://doi.org/10.3174/ajnr.A0772>

<http://www.ajnr.org/content/28/10/2001>

# 3D Time-Resolved Contrast-Enhanced Cerebrovascular MR Angiography with Subsecond Frame Update Times Using Radial $k$ -Space Trajectories and Highly Constrained Projection Reconstruction

## TECHNICAL NOTE

Y. Wu  
N. Kim  
F.R. Korosec  
A. Turk  
H.A. Rowley  
O. Wieben  
C.A. Mistretta  
P.A. Turski

**SUMMARY:** HYPR TRICKS is an acquisition method that combines radial  $k$ -space trajectories, sampling  $k$ -space at different rates (TRICKS), and a new strategy for image reconstruction that uses highly constrained backprojection reconstruction (HYPR). This approach provides 3D time-resolved contrast-enhanced MR angiograms of the cerebral vessels with subsecond frame update times and submillimeter in-plane spatial resolution. Artifacts are suppressed, and signal-to-noise ratio is well maintained, by using HYPR reconstruction.

For several decades, time-resolved serial imaging using x-ray digital subtraction angiography has played a major role in the diagnosis of vascular disease.<sup>1</sup> A new group of time-resolved contrast-enhanced MR angiographic techniques is emerging<sup>2</sup> that generates a series of datasets with adequate temporal resolution to capture arterial, mixed, and venous-phase images during the passage of a contrast agent through the cerebrovascular system.<sup>3</sup> Initial investigations used 2D techniques.<sup>4,5</sup> This was later extended to 3D serial acquisitions.<sup>6–8</sup> Time-resolved contrast-enhanced MR angiography is essential for the characterization of high-flow lesions<sup>9,10</sup> such as arteriovenous malformations (AVMs) and dural fistulas.<sup>11,12</sup>

Recently an innovative reconstruction method that uses highly constrained backprojection reconstruction (HYPR) was introduced to reduce the undersampling artifacts from radial acquisition and maintain good signal-to-noise ratio (SNR) even at high levels of acceleration. Fig 1 shows a series of highly undersampled radial trajectories, in which the orientation of the trajectories in each set is different from the orientations of the trajectories in all the other datasets. If each image is reconstructed by using conventional filtered backprojection, streak artifacts degrade the image as demonstrated in Fig 1 (top row). The data in each image are unique, and multiple images can be combined to form a more fully sampled dataset called the composite image. Because the composite image is produced by using data acquired during a longer duration than a single image, it contains temporal information from a longer time interval than a single frame. The more frames of

data combined to produce the composite image, the fewer the artifacts and the higher the SNR but the poorer the temporal characteristics.

A temporal weighting image is produced by using the data from each timeframe to restore the temporal characteristics. The weighting images are produced by backprojecting the normalized data acquired for each timeframe. Because data spanning only a single timeframe are used to produce the weighting image, the temporal characteristics of the weighting image are well maintained.

The weighting image (which contains good temporal characteristics but poor spatial resolution) is multiplied by the composite image (which contains few artifacts, good SNR, and good spatial resolution, but poor temporal characteristics) to produce the final HYPR image. The resulting HYPR timeframes have good spatial resolution and good temporal characteristics.

In this article, HYPR was used in conjunction with the hybrid radial/Cartesian acquisition to simultaneously achieve high temporal and spatial resolution. The components of HYPR time-resolved imaging of contrast kinetics (TRICKS) are the following: 1) sampling  $k_x$ - and  $k_y$ -space along radial rather than traditional rectilinear trajectories, 2) sampling the lower spatial frequencies more often than the higher spatial frequencies, and 3) using HYPR to reduce artifacts and SNR loss typically associated with undersampling methods. Combining HYPR reconstruction with these 2 elements enables the use of even greater undersampling factors, permitting generation of a series of 3D datasets with subsecond frame update times and submillimeter in-plane resolution.

## Methods and Subjects

For this study, the HYPR TRICKS method was used to acquire 3D time-resolved contrast-enhanced MR angiograms of the cerebral vessels in 14 healthy subjects and 2 patients with AVMs, by using a protocol that was approved by the institutional review board. For 4 of the 14 healthy subjects and the 2 patients with AVMs, HYPR TRICKS and Cartesian TRICKS examinations were performed during separate injections.

Received March 5, 2007; accepted after revision June 4.

From the Departments of Radiology (N.K., F.R.K., A.T., H.A.R., C.A.M., P.A.T.) and Medical Physics (Y.W., F.R.K., O.W., C.A.M.), University of Wisconsin School of Medicine and Public Health, Madison, Wis.

This work was supported by: the National Institutes of Health grants 2R01HL072260-05 and R21EB006393-01.

Please address correspondence to Patrick A. Turski, MD, Department of Radiology, University of Wisconsin Hospitals and Clinics, Clinical Science Center, 600 Highland Ave, E3/398, Madison, WI 53792; e-mail: PTurski@UWHealth.org

DOI 10.3174/ajnr.A0772

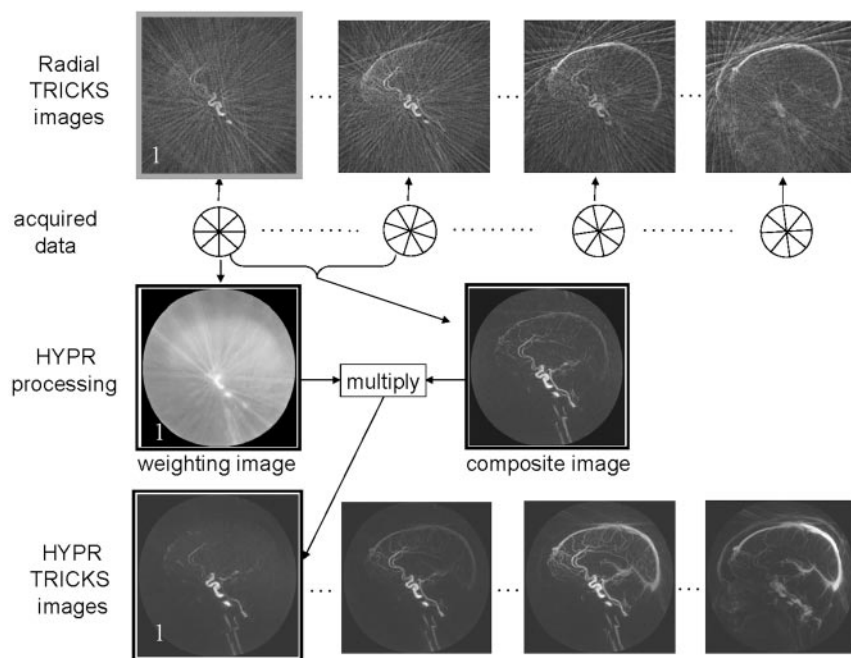


**Fig 1.** Schematic diagram of the HYPR reconstruction algorithm. Data were acquired by using undersampled radial trajectories. Images in the top row were reconstructed by using filtered backprojection. Images in the bottom row were reconstructed by using the HYPR method. All processing was performed on the source images, and the resulting maximum-intensity-projection images are shown. The low attenuation of vessels (high sparsity) in the source images makes them amenable to HYPR processing. For the HYPR processing, note that the sagittal sinus that appears in the composite image is suppressed following multiplication by the weighting image for frame 1.

For the HYPR TRICKS method, a 3D gradient-echo sequence was modified to sample data along radial trajectories in the  $k_x$ - $k_y$  plane, and multiple planes of data were sampled in the  $k_z$  direction by using traditional partition encoding. Angular undersampling was applied to the radial trajectories that formed each timeframe such that the number of radial lines per frame,  $N_r$ , was much smaller than that which is traditionally understood to be the minimum necessary to accurately reconstruct the object being imaged (the Nyquist sampling criterion). These  $N_r$  radial lines were evenly distributed over a full circle in the  $k_x$ - $k_y$  plane for each frame. The orientation of the group of radial lines was rotated from one frame to the next. The rotation angle was chosen so that data for the current frame best filled in the gaps left after combining data from all the previous frames.<sup>13</sup> When all the gaps were filled in such that a fully-sampled dataset could be formed by combining all of the acquired data, then the sampling pattern was repeated.

Data in the  $k_z$  direction were sampled by using the TRICKS acquisition method. For this implementation,  $k_z$  was divided into 3 regions; a central region A was sampled more frequently than the peripheral B and C regions.

HYPR TRICKS studies were performed on 1.5T ( $n = 5$ ) and 3T ( $n = 11$ ) MR imaging scanners (Signa HD; GE Healthcare, Milwaukee, Wis). On 4 healthy subjects and 2 patients with AVMs, 2 acquisition methods, HYPR TRICKS and Cartesian TRICKS, were performed on the 3T scanner during a 1-hour scanning session with approximately a 20-minute interval between the 2 injections. The ordering of the scans was such that the HYPR TRICKS method was performed first in 2 of the 4 healthy subjects and 1 patient and the Cartesian TRICKS method was performed first in the other 2 healthy subjects and the other patient. Typical imaging parameters for the HYPR TRICKS and Cartesian TRICKS were the following: TE/TR, 1.1/6.6 ms for HYPR TRICKS and 1.6/4.4 ms for Cartesian TRICKS; readout points per TR, 512 for HYPR TRICKS and 256 for Cartesian TRICKS; 10–14 projections per section for HYPR TRICKS and 120 phase-encoding lines per section for Cartesian TRICKS. FOVs were  $240 \times 240 \times 48 \text{ mm}^3$  for both methods. The dose of contrast material (gadodiamide [Omniscan; GE Bioscience, Princeton NJ]) was 0.1

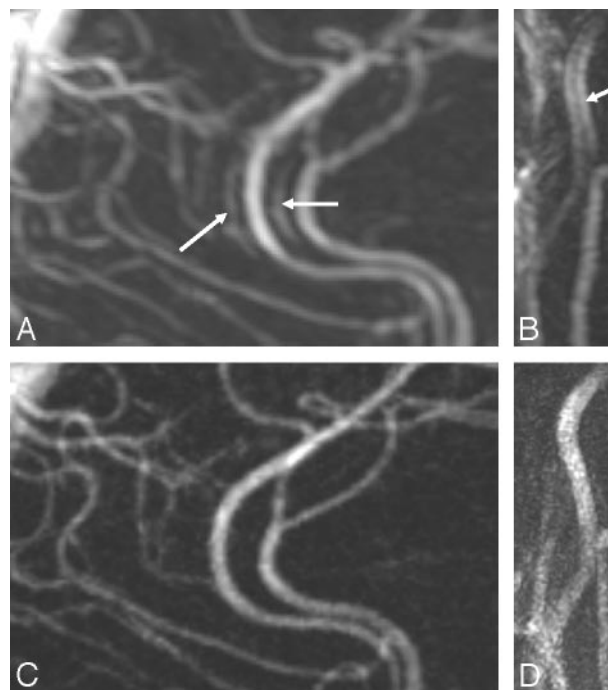


**Fig 2.** Comparison of in-plane resolution and artifacts for Cartesian TRICKS ( $0.94 \times 1.5 \text{ mm}$ ) (A, B) and HYPR TRICKS ( $0.47 \times 0.47 \text{ mm}$ ) (C, D). Arrows in the Cartesian TRICKS images show the ghosting and black band artifacts resulting from fluctuations in signal intensity occurring during acquisition of data for a single frame, caused by changes in the concentration of contrast material. More rapid and larger fluctuations lead to more severe artifacts.

mg/kg of body weight. It was injected at a rate of 2–3 mL/s by using an automated power injector (Spectris; Medrad, Indianola, Pa). Administration of the contrast material was followed immediately by a 25-mL saline flush injected at the same rate as that of the contrast material.

## Results

The combination of radial  $k$ -space trajectories and HYPR image reconstruction resulted in radial undersampling factors up

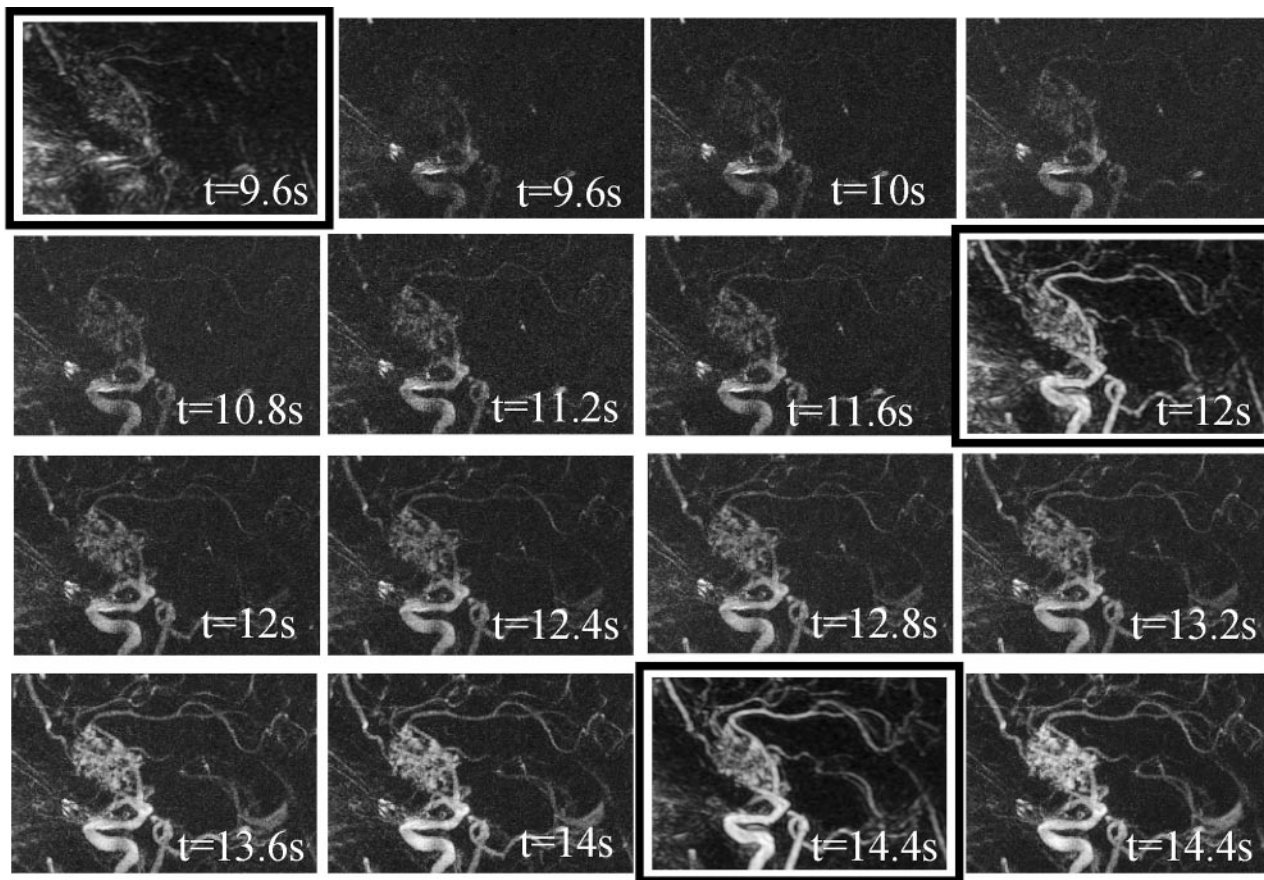


**Fig 3.** Comparison of Cartesian TRICKS timeframes (the 3 images with the black frames) and HYPR TRICKS timeframes from a patient with AVM. The frame update times are 0.4 seconds for HYPR TRICKS and 2.4 seconds for Cartesian TRICKS.

to 80 relative to Nyquist requirements (10 versus 804 radial lines), which, when combined with TRICKS temporal undersampling factor of 3, provided an overall undersampling (or acceleration) factor of 240 relative to a conventional fully sampled radial acquisition. When compared with the current commercially available Cartesian TRICKS examination, HYPR TRICKS achieved the temporal acceleration factor of approximately 10 (0.26-seconds frame update time versus 2.4 seconds) with the improved spatial resolution by a factor up to 3 ( $0.47 \times 0.47 \times 4 = 0.88 \text{ mm}^3$  versus  $0.94 \times 1.5 \times 2 = 2.8 \text{ mm}^3$ ).

Fig 2 demonstrates that even with a 10-fold increase in temporal update rate, HYPR TRICKS allows a factor of 3 decrease in voxel volume relative to that provided by the commercially available Cartesian TRICKS method. Although the loss in SNR expected with the achieved acceleration should be a factor of approximately 9.5 (square root of  $10 \times 3 \sim 9.5$ ) based on the reduced voxel volume (SNR reduction factor = 3) and the reduced temporal acquisition window (SNR reduction factor = square root of 10), the SNR measured in the HYPR TRICKS images was reduced by only a factor of 2 relative to the SNR measured from the Cartesian TRICKS images. This reduced SNR interferes, to some extent, with the ability to fully appreciate the smaller voxels provided by HYPR TRICKS. However, despite this, there is a perceived increase in vessel definition.

Fig 2 also demonstrates artifacts in the Cartesian TRICKS image (arrows). When data are acquired during the arrival and

passage of contrast material,  $k$ -space data are modulated by a time-dependent intensity variation, which leads to ghosts originating from the vessels (Fig 2A) or the appearance of a dark band running along the middle of the vessels (Fig 2B) in the reconstructed images.<sup>14</sup> In Cartesian imaging, these ghosts are coherent and appear as “ringing” or replication of the vessels. With HYPR TRICKS, the reconstruction window is 10 times shorter in duration than in Cartesian TRICKS, leading to far less modulation and, therefore, far fewer artifacts in the HYPR TRICKS images. In addition, any artifacts that would result from modulation of the signal intensity during acquisition of the HYPR TRICKS data would be incoherently distributed throughout the image due to the radial acquisition process.

Results obtained from a patient with an AVM are shown in Fig 3. In Fig 3, a series of HYPR TRICKS images demonstrate the contrast material passing from the feeding arteries, through the nidus, and into the draining veins of the AVM. Acquired over a similar period of time during a separate injection of contrast material, 3 Cartesian TRICKS images (also shown in Fig 3) do not capture the early and intermediate phases of contrast material passage.

## Discussion

Achieving high spatial and temporal resolution simultaneously is extremely difficult with the currently predominant methods that use Cartesian  $k$ -space acquisitions. In this investigation, radial  $k$ -space was vastly undersampled, but streak



Acceleration comparison of HYPR TRICKS with different 3D imaging techniques					
	3D Hybrid	3D CART	512-TRICKS	CLTRICKS	HYPRTRICKS
$N_p^a$	$512 \times \pi/2$	512	512	$120^b$	10
$N_z$	$N_z$	$N_z$	$N_z/3$	$2 \times N_z / 4$	$N_z/3$
$f_a$	$80 \times 3 = 240$	$51 \times 3 = 153$	51	$29^c$	1

**Note:**— $N_z$  indicates the number of sections;  $f_a$ , the acceleration factor of HYPR TRICKS versus the corresponding technique, which is ratio of  $N_p \times N_z$  from the 2 techniques; 3D Hybrid, 3D radial in-plane and Cartesian through-plane technique; 3D CART, 3D Cartesian technique full Nyquist sampling; 512-TRICKS, 3D Cartesian TRICKS with the same spatial resolution as HYPR TRICKS without partial Fourier, rectangular FOV, etc; CLTRICKS, clinically used 3D Cartesian TRICKS that is described in the article. Parameters chosen in the article were based on the clinical protocol.

<sup>a</sup> Where  $N_p$  is the number of encodings per timeframe in the  $k_x$ - $k_y$  plane. For radial imaging, it is the number of projections per timeframe, and for the Cartesian imaging, it is the number of phased-encoding lines per timeframe.

<sup>b</sup> Partial Fourier and rectangular FOV techniques were applied, given the in-plane pixel size 6 times larger than that achieved by the HYPR TRICKS.

<sup>c</sup> This factor was calculated on the basis of the ratio of the actual frame update time (2.4 seconds versus 0.26 seconds) together with the ratio of the voxel size (2.8 mm<sup>3</sup> versus 0.88 mm<sup>3</sup>).

artifacts were suppressed by using HYPR reconstruction. For the HYPR work described here, 10 projections were acquired per time frame, giving a temporal acceleration factor of approximately 51 relative to a conventional Cartesian MR imaging with equivalent in-plane resolution (10 projections versus 512 phase encodings, assuming no additional acceleration methods such as parallel imaging, partial Fourier acquisition, or rectangular FOV) or an undersampling factor of 80 relative to a fully sampled radial acquisition. Acceleration factors for HYPR TRICKS are summarized for hybrid and Cartesian techniques in the Table. Furthermore, the SNR was well maintained in the HYPR images, despite the large undersampling factors. Because the signal intensity in the timeframe (weighting image) projections came from summing all of the signals along the projection direction, the SNR in the weighting image is very high. Therefore, it is not the weighting image but the composite image that determines the SNR in the HYPR images. This is a significant departure from conventional SNR behavior, in which the SNR is directly proportional to the square root of the number of samples acquired. The consequence is high SNR even in timeframes having very high temporal and spatial resolution.

HYPR is optimal when the signal intensity-producing sources are sparse and spaced far apart (ie, vascular structure). The vast undersampling of the weighting images may become problematic when vessels that enhance at different times are both present in the composite image and they are very near each other. In this case, when the composite image is multiplied by the undersampled weighting image, the weighting from 1 vessel may overlap onto a very close vessel, causing it to have the improper intensity in the final HYPR image. Therefore, when vessels are very proximal to each other, it may be advantageous to limit the amount of data to a window of acquisition centered on the frame of interest. This reduces the temporal window of the composite image, and limits the inclusion of vessels that enhance at different times.

## Conclusions

The results in 14 healthy volunteers and 2 patients with AVMs confirm that HYPR TRICKS is able to generate subsecond 3D time-resolved contrast-enhanced cerebrovascular MR angiograms with submillimeter in-plane spatial resolution that permits separation of arterial and venous structures in images with minimal artifacts.

## References

1. Kwan ES, Hall A, Enzmann DR. Quantitative analysis of intracranial circulation using rapid-sequence DSA. *AJR Am J Roentgenol* 1986;146:1239–45
2. Wetzel SG, Bilecen D, Lyrer P, et al. Cerebral dural arteriovenous fistulas: detection by dynamic MR projection angiography. *AJR Am J Roentgenol* 2000;174:1293–95
3. Griffiths PD, Hoggard N, Warren DJ, et al. Brain arteriovenous malformations: assessment with dynamic MR digital subtraction angiography. *AJNR Am J Neuroradiol* 2000;21:1892–99
4. Hans FJ, Reinges MH, Reipke P, et al. Clinical applications of 2-D dynamic contrast-enhanced MR subtraction angiography in neurosurgery: preliminary results. *Zentralbl Neurochir* 2005;66:170–79
5. Nagaraja S, Capener D, Coley SC, et al. Brain arteriovenous malformations: measurement of nidus volume using a combination of static and dynamic magnetic resonance angiography techniques. *Neuroradiology* 2005;47:387–92
6. Korosec FR, Frayne R, Grist TM, et al. Time-resolved contrast-enhanced 3D MR angiography. *Magn Reson Med* 1996;36:345–51
7. Carroll TJ, Korosec FR, Pertermann GM, et al. Carotid bifurcation: evaluation of time-resolved three-dimensional contrast-enhanced MR angiography. *Radiology* 2001;220:525–32
8. Cashen TA, Carr JC, Shin W, et al. Intracranial time-resolved contrast-enhanced MR angiography at 3T. *AJNR Am J Neuroradiol* 2006;27:822–29
9. Farb RI, McGregor C, Kim JK, et al. Intracranial arteriovenous malformations: real-time auto-triggered elliptic centric-ordered 3D gadolinium-enhanced MR angiography: initial assessment. *Radiology* 2001;220:244–51
10. Duran M, Schoenberg SO, Yuh WT, et al. Cerebral arteriovenous malformations: morphologic evaluation by ultrashort 3D gadolinium-enhanced MR angiography. *Eur Radiol* 2002;12:2957–64
11. Gaurvit JY, LeClerc X, Oppenheim C, et al. Three-dimensional dynamic MR digital subtraction angiography using sensitivity encoding for the evaluation of intracranial arteriovenous malformations: a preliminary study. *AJNR Am J Neuroradiol* 2005;26:1525–31
12. Nael K, Michael H, Villablanca P, et al. Time-resolved contrast-enhanced magnetic resonance angiography of the head and neck at 3.0 tesla: initial results. *Invest Radiol* 2006;41:116–24
13. Rabiner LR, Gold B. *Theory and Application of Digital Signal Processing*. Englewood Cliffs, NJ: Prentice-Hall Inc; 1975:chaps 6 and 10, 365, 578
14. Maki JH, Prince MR, Londy FJ, et al. The effects of time varying intravascular signal intensity and k-space acquisition order on three-dimensional MR angiography image quality. *J Magn Reson Imaging* 1996;6:642–51